Assessing land cover changes in the cedar and fir protected area/Syria using Sentinel 2A satellite data and the google earth engine platform

Ola Ali Merhej[1*]

[1] General Organization of Remote Sensing (GORS), Lecturer- Tishreen University, Latakia, Syria.

(*Corresponding author: Ola Merhej, Email: olamerhej@gmail.com, mobile: 0932044199)

Received: 6/ 2/ 2025 **Accepted:** 15/ 6/ 2025

Abstract

The rapid change in land cover has become a major problem resulting from various factors in the Cedar and Fir protected area in Syria, even though it is under protection. This study aimed at evaluating the usefulness of monitoring changes in land cover in the Cedar and Fir protected area in Syria during the last 5 years (2018-2023), using two imageries from the Sentinel-2A (S2A) satellite and applying the Random Forest "RF" algorithm within Google Earth Engine (GEE) platform. The overall accuracy (OA) of classification in the resulting land cover maps was 93.4% in the 2018 map, and 92.7% in the 2023 map. The maps showed a decrease in forest cover in the protected area by 36.07% during the study period. In contrast, the results strongly support the use of the GEE platform and Sentinel 2A satellite data in parallel with the random forest algorithm to enhance the accuracy of land cover classification in mountainous regions. This study recommended the need to take rapid action to preserve the rare natural resources in the protected area.

Keywords: Cedar and Fir Protected Area, Google Earth Engine Platform, Random Forest, Remote Sensing, Land Cover Maps.

INTRODUCTION:

Land use/land cover (LULC) changes globally due to natural and anthropogenic causes; consequently, local communities are affected by land cover changes. It is essential and crucial to obtain reliable and accurate spatio-temporal information about land use and land cover in mountainous areas. Many restrictions are put in Syria on the use of high-resolution satellite images such as Satellite Pour l'Observation de la Terre (SPOT) data. However, lower-resolution (medium spatial resolution) image data such as LANDSAT and Sentinel 2A are available most of the time. for this reason, using this data efficiently to produce the best product that can be used and benefited from in various applications was important. Lately, great interest in applying machine learning algorithms to remote sensing images for LULC mapping has increased (Maxwell et al., 2018). Moreover, Support Vector Machine (SVM), RF and other models, which are more advanced methods, have become the focus of exceptional interest in applications based on remote sensing, such as LULC classification (Talukdar et al., 2020; Zhang et al., 2019; Teluguntla et al., 2018).

One of the most widely used machine learning algorithms is the Random Forest "RF" model (Woznicki et al., 2019), as it is an intelligent and versatile machine learning technique that is able to perform classification and regression tasks using a statistical technique and several decision trees for the production of more stable and accurate predictions. (Biau and Scornet, 2016).

When compared to other classifiers, such as Maximum Likelihood Classification (MLC), Artificial Neural Network (ANN) and SVM, the advantages of RF are quite efficient in processing large multi-source data sets, in addition to dealing with a large number of input variables without variable deletion, and require less time for model training (Belgiu and Drăguţ, 2016).

For the management and analysis of satellite datasets in recent years, it has been observed that Google Earth Engine (GEE) is increasingly used in land use and cadastral studies (Amani et al., 2020; Tamiminia et al., 2020). GEE is a free cloud computing platform that uses JavaScript code for planet-scale geospatial analyses. It is useful for processing and using large data sets (Gorelick et al., 2017). GEE also provides huge amounts of global time series satellite imagery, such as daily MODIS data, Landsat archives which date back to the early 1980s, Sentinel-1 (S1) data and Sentinel-2A images (Kumar and Mutanga, 2018).

In order to generate land use and land cover maps for forests that are situated in the northwestern Syria, Multi-temporal Landsat data have been applied using supervised classification and MLC algorithm (Merhej et al., 2021). The study reached consistent and efficient overall classification, and it achieved a classification accuracy of over 85% (Merhej et al., 2021).

GEE is not widely used in Syria in the land cover classification process to the researcher's knowledge, which makes the use of multi-sensor satellite data and the GEE platform face a challenge when conducting a robust, long-term, real-time operational monitoring of land cover in Syria. Based on the above-mentioned, this study aimed at evaluating land cover changes in the Cedar and Fir protected area during the period that extends from 2018 to 2023 using S2A satellite data by using a Random Forest "RF" classifier together with the GEE platform.

MATERIALS AND METHODS:

1. Study Area

The research was conducted in the summer of 2023 in the Cedars and Fir protected area in Syria to assess land cover changes in the reserve three years after the 2020 fire.

The study area is situated in the coastal mountains in north-western Syria, on the western and eastern slopes of Mount Nabi Matta, in Slenfa district of Latakia Governorate. The region is situated between latitudes 35.41 and 35.29 north, and longitudes 36.10 and 36.17 east, Figure (1).

The area's elevation above sea level ranges between 900 and 1560 meters; its lowest point is located at the Jubb al-Shuh site on the high-slope eastern side, with a slope of 35 degrees, while the slope of the western side ranges between 20 and 27 degrees. The climate of cedar and fir forests, which fall within the very humid and cool bioclimate zone, is typical Mediterranean. The average annual precipitation ranges between 1390 and 2092 mm/year.

The dominant type on the eastern slope is *Cedrus libani*, while the dominant type on the western slope is Abies cilica. Other types can also be found, such as *Quercus cerris* sub. *pseudocerris*, *Juniperus oxycedrus*, and others. Some small villages are situated on the eastern and western edges of the protected area. The reserve lost a huge amount of forest cover on the eastern slope of the reserve due to a major fire between September 5 and 9, 2020, and the majority of this forest cover is Cedar.

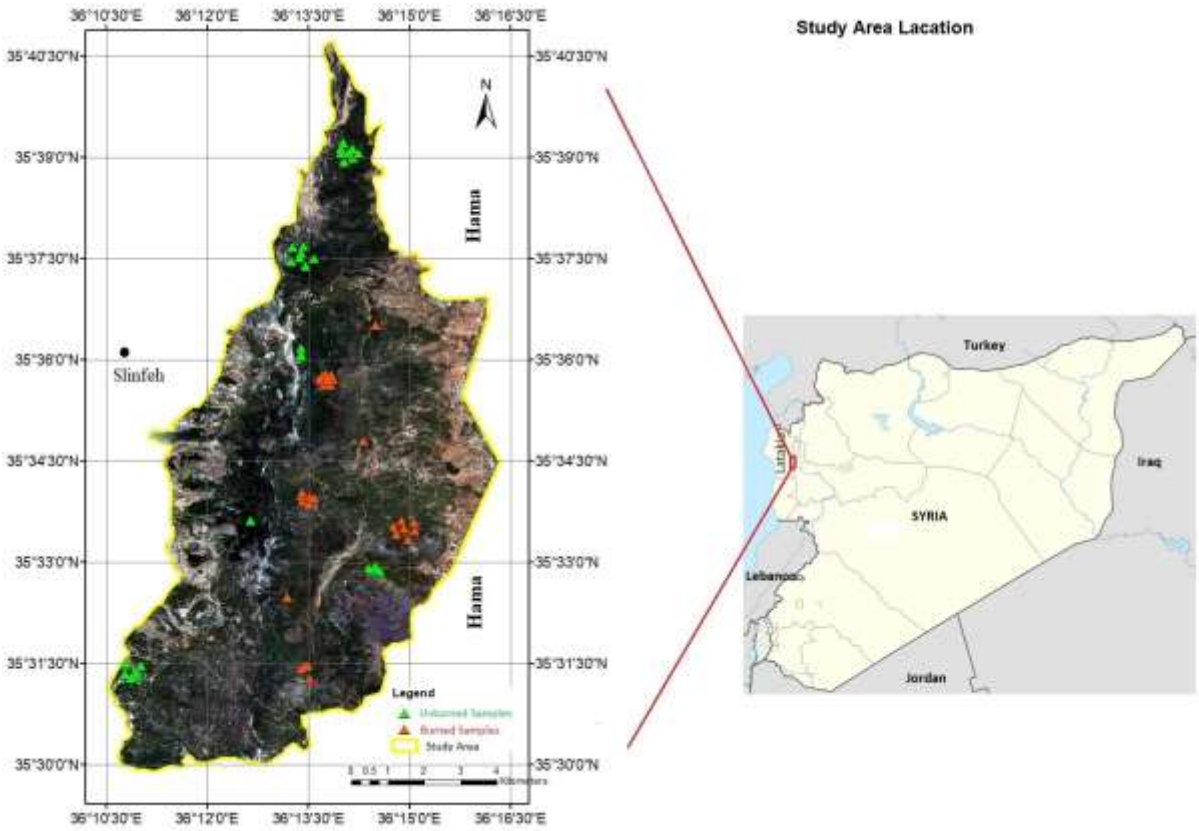

Fig. (1): Study area location

2. *Data set*

Data from Sentinel 2A satellite was used in this study. The data includes an image obtained in August 2018 and another in August 2023 with almost non-existent cloud coverage of the study area so that changes in land cover resulting from the difference in season can be avoided and to also obtain images without clouds.

3. *Methodology*

The researcher visited the area several times before and after the 2020 fire, and this enabled the characteristics and types of land cover at the study site to be identified by the researcher. The study uses four main land cover categories: urban area, forest, non-forest vegetation (which includes agricultural land, maqui, and post fire vegetation), rocks and bare soil (Rock_baresoil). Using visual interpretation of high-resolution Google Earth images, regions of interest (ROIs) for each LULC class were identified; this was based on advanced knowledge of land cover data acquired through previous and ongoing field work (Liu et al., 2018; Sarzynski et al., 2020).

A simplified workflow of the work steps that were adopted in this study are shown in figure (2). They are:

a) **Pre-processing:** The two images were retrieved with L2 correction level; ie. reflectance from the GEE repository. All selected satellite data for the first image were calculated for the two years studied, which were clipped at the boundaries of the study area.

b) Image classification and change detection: Using an RF-supervised machine learning algorithm and the GEE platform to produce land cover maps for 2018 and 2023, each image was individually classified into four land cover classes.

In order to provide a reliable estimate of error and conserve computation times, the number of classification trees required was set to 10. The number of predictor variables used to split a node was set at the square root of the number of input variables (Cutler et al., 2007).

In order to harmonize the different datasets, all input data were resampled to 10 m resolution using cubic interpolation (Vizzari, 2022; De Luca et al., 2022).

LULC changes were determined by applying the 2018–2023 post classification comparison method (Tewkesbury et al., 2015).

c) Accuracy Assessment: Through using a confusion matrix, which has been adopted as the standard descriptive reporting tool for assessing accuracy, LULC classification accuracy assessment was performed (Congalton and Green, 2019). The study randomly selected a set of ground control points and stratified random sampling based on high resolution Google Earth images in order to train the RF classifier (80% of the pixels from each LULC class) and to validate the samples (the remaining 20% of the pixels) (Belgiu and Drăguţ, 2016).

In order to calculate kappa coefficient (K), overall accuracy (OA), user's accuracy (UA), and producer's accuracy (PA), the confusion matrix was used. The Kappa coefficient is a measure of the performance of an RF algorithm, and the possible K values range from -1 (very poor fit) to 1 (excellent fit). The overall accuracy values represent the average percentage of the range of correctly classified pixels from 0 (no pixels are correctly classified) to 1 (100% of pixels are correctly classified). Product accuracy is a measure of omission error (underestimation) while user accuracy is a measure of commission error (Story and Congalton, 1986).

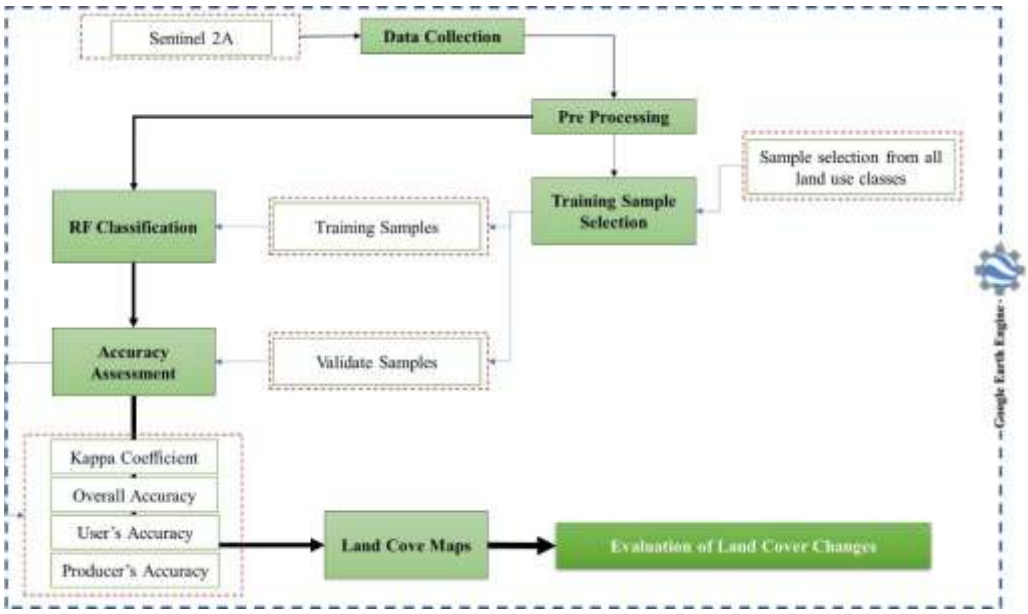

Fig. (2): Data processing flow chart

RESULTS AND DISCUSSION:

This study demonstrated the potential of Sentinel 2A satellite data to monitor LULC changes in the

Cedar and Fir Reserve, and the land cover maps for the two years studied are shown in Figure (3).

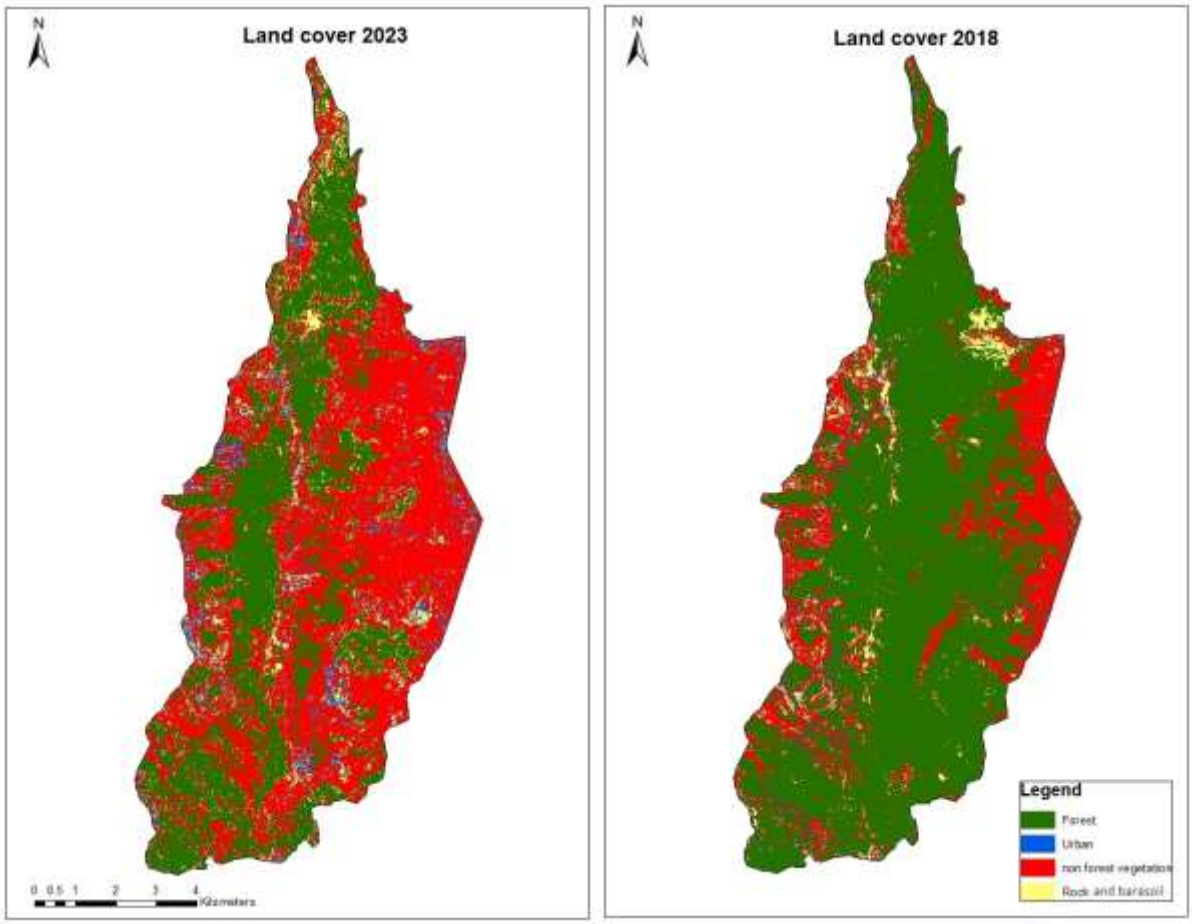

Fig. (3): Land cover maps for 2018 and 2023 using RF

Considering Figure (3), we note the clear regression of the forest class from the eastern half of the study area and the expansion of the non-forest vegetation class as an alternative. Very good kappa coefficient values of 0.91 in the 2023 map and 0.87 in the 2018 map were given after combining the spectral bands which are available in the S2A satellite data. On the other hand, the overall accuracy reached 93.4% in the 2018 map and 92%. 7% in the 2023 map. This leads to the following conclusion: the classification that uses the RF model and the GEE platform is more accurate than the one that uses the MLC maximum likelihood classification model which is applied in the forests of northern Latakia (Bayer and Bassit) using the Erdas Imagine software (Merhej, 2020).

The producer accuracy (PA) and user accuracy (UA) values for each land cover class ranged from 0.51 to 1 for the PA and from 0.75 to 0.97 for the UA. Low values were generally in the "bare soil and rock" class, which may be due to spectral confusion resulting from the convergence of spectral reflectance values between this class and the class of urban (Yang, 2002).

In the same context, GEE allows fast processing of multi-sensor satellite data, since image downloading and local data storage are not necessary. In contrast, many government agencies interested in environmental matters such as monitoring land cover change that publish official national reports on natural resources, use traditional operational image processing techniques requiring expensive hardware and special software.

Table (1) shows percentage distribution and details of the area derived from maps for each land cover class.

Table (1): Area (hectares) and percentage of land cover classes in the Cedar and Fir Reserve during the study period.

Class	2018		2023	
	area	percentage	area	**percentage**
Forest	6435.32	72.78	3245.81	**36.71**
Urban	172.17	1.95	356.61	**4.03**
non forest	1867.23	21.12	4577.03	**51.76**
Rock bare soil	367.27	4.15	662.54	**7.49**

The main land cover type in 2018 was forest with an area that made up (72.81%) of the total area of the reserve, and this is logical since the study area is a protected area established for preserving the two types of cedar and fir. The forest area decreased from 6423.73 hectares in 2018 to 2851.07 hectares in 2023 (Table 1). It is clear that the main reason for the regression in the forest area in the study area is the 2020 fire, which reached an area of 2,495 hectares (Merhej, 2023), with the forest cover not being adequately renewed.

The agricultural areas were concentrated around the villages situated on the eastern and western outskirts of the reserve (Figure (3)), and an increase in non-forest vegetation areas was reported due to the death of trees and the growth of post-fire plants such as sycamore and others, with the burnt cedar not returning, as the area of the non-forest vegetation class was 1867.23 hectares in 2018 and it increased to 4577.03 hectares in 2023. The percentage change in each land cover class is shown in Figure (4), where the decrease in the forest class was the only decrease that occurred among the land cover classes in the Cedar and Fir Reserve by 36.07%, compared to a basic increase in the non-forest vegetation class by 30.65 % and a smaller increase in the other two classes. Rocks-bare soil and urban area classes with ratios of 3.34% and 2.09%, respectively.

In the study area, the environmental measures implemented by the reserve administration, such as activating partnership between the forest and the local community and spreading awareness of the importance of the forest, were insufficient taking into consideration the economic conditions experienced in the country during the last decade, which reduced awareness of sustainable use practices and increased random practices of using the forest. Many people have switched from all firewood, dead and diseased trunks and pruning operations to cutting down old trees, from using firewood for heating to charcoal, and from collecting bay leaves to cutting down entire trees after the export of bay leaves was promoted to gain more income and improve their quality of life (Local newspapers and websites, 2023).

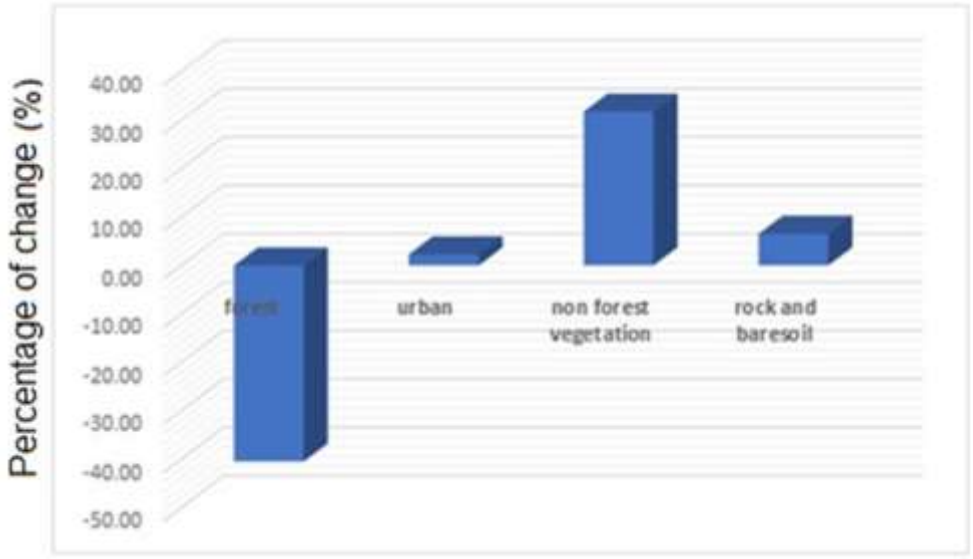

Fig. (4): Percentage change in land cover classes between 2018 and 2023

Although changes in the forest are high in the reserve, the western slope, which is managed by the local community in cooperation with the Forestry Department in Latakia, is noted to have been well preserved due to the community's strong protection from deforestation, which is the main key to managing natural resources, especially in forest areas, for sustainable land use and management.

CONCLUSION:

This study represents the first assessment of land cover change in the Cedar and Shuh Reserve during the Syrian war, with a focus on the recent years in which the reserve was exposed to the most impactful practices. An evaluation of the potential of Sentinel 2A satellite data to produce maps of land cover change in 2018 and 2023 was performed using the RF random forest model and the GEE cloud computing platform. This study highlighted the advantages of an RF classifier in conjunction with the GEE platform that can display great performance in fast processing of multi-sensor satellite data and the ability to handle high-dimensional data. It is clearly useful to use the GEE platform to assess change in LULC for rating purposes and it can be used for the benefit of the operational rating process. An overall accuracy using the spectral bands of Sentinel- 2A images exceeding 90% was achieved. On the other hand, classification must be enhanced by adding field verification points from the eastern slope to enable differentiation between herbaceous forest plants and agricultural crops that give close spectral reflectance.

Regarding the reserve management policies in place, forest areas revealed widespread encroachments in the reserve during the study period, mainly caused by the 2020 fire. Having the forest cover not beginning to return even three years after the fire makes us sound the alarm and urgently requires taking more effective measures to protect the remaining trees of the reserve, especially the Lebanese cedar.

Geoinformatics and remote sensing technology will provide the possibility of monitoring the reserve's response to established plans and thus assessing and monitoring the impact of established policies.

REFERENCES:

Amani M, Ghorbanian A, Ahmadi SA, Kakooei M, Moghimi A, Mirmazloumi SM, et al. (2020). Google earth engine cloud computing platform for remote sensing big data applications: A comprehensive review. IEEE Journal of Selected Topics in Applied Earth Observations and Remote Sensing.13: 5326-50. DOI: https://doi.org/10.1109/JSTARS.2020.3021052

Belgiu M, Drăguţ L. (2016). Random Forest in remote sensing: A review of applications and future directions. ISPRS Journal of Photogrammetry and Remote Sensing. 114: 24-31. DOI: https://doi.org/10.1016/j.isprsjprs.2016.01.011

Biau G, Scornet E. (2016). A random forest guided tour. TEST. 25(2):197-227. DOI: https://doi.org/10.48550/arXiv.1511.05741

Campbell JB, Wynne RH. (2011). Introduction to Remote Sensing. New York, USA: Guilford Press.

Congalton RG, Green K. (2019). Assessing the Accuracy of Remotely Sensed Data: Principles and Practices, 3rd ed. Boca Raton, USA: CRC Press.

Cutler DR, Edwards TC, Beard KH, Cutler A, Hess KT, Gibson J, et al. (2007). Random forests for classification in ecology. Ecology. 88(11): 2783-92. DOI: https://doi.org/10.1890/07-0539.1

De Luca G, M.N. Silva J, Di Fazio S, Modica G. (2022). Integrated use of Sentinel-1 and Sentinel-2 data and open-source machine learning algorithms for land cover mapping in a Mediterranean region. European Journal of Remote Sensing. 55(1): 52-70. DOI: https://doi.org/10.1080/22797254.2021.2018667

Gorelick N, Hancher M, Dixon M, Ilyushchenko S, Thau D, Moore R. (2017). Google Earth Engine: Planetary-scale geospatial analysis for everyone. Remote Sensing of Environment. 202: 18-27. DOI: https://doi.org/10.1016/j.rse.2017.06.031

Kumar L, Mutanga O. (2018). Google Earth Engine applications since inception: Usage, trends, and potential. Remote Sensing. 10(10): Article No. 1509. DOI: https://doi.org/10.3390/rs10101509

Liu X, Hu G, Chen Y, Li X, Xu X, Li S, et al. (2018). High-resolution multi-temporal mapping of global urban land using Landsat images based on the Google Earth Engine Platform. Remote Sensing of Environment. 209: 227-39. DOI: https://doi.org/10.1016/j.rse.2018.02.055

Maxwell, A.E.; Warner, T.A.; Fang, F. (2018). Implementation of machine-learning classification in remote sensing: An applied review. Int. J. Remote Sensing. 39: 2784–2817. DOI: https://doi.org/10.1080/01431161.2018.1433343

Merhej, O.A.; Ali, M.; Thabeet, A. and Idriss, Y. (2021). Land Use/ Land Cover Change Detection in Baer and al- Bassit Region, Latakia, Syria during the Period of 1972- 2018. Scientific J King Faisal University (Basic and Applied Sciences). 2(22): 20-25. DOI: https://doi.org/10.37575/b/sci/2070

Merhej, Ola. (2023). Evaluation of Several Spectral Indices to Produce Post Fire Maps (Case Study: Cedar-Fir Protected Area, Syria). Syrian Journal of Agriculture Research (ISSN: 2410- 3608). 10(1): 284-294. Available at: https://agri-research-journal.net/SjarEn/?p=6287 (Accessed on 12 June 2024)

Merhej, Ola. (2020). Evaluation of land use changes and fire risk in Al-Bayer and Al-Bassit forests (Latakia Governorate) during the period 1977-2017 using remote sensing techniques and geographic information systems. doctoral thesis submitted to the Department of Forestry and Environment - Faculty of Agriculture - Tishreen University. P 127. (In Arabic). Available at: https://www.researchgate.net/publication/342492959_Evaluating_land_use_changes_and_danger_of_fires_on_Bayer_and_al-Bassit_Forest_Lattakia_Province_during_the_period_1977-2017_using_remote_sensing_and_GIS_technologies (Accessed on 10 June 2024)

Sarzynski T, Giam X, Carrasco L, Lee JSH. (2020). Combining radar and optical imagery to map oil palm plantations in Sumatra, Indonesia, using the Google Earth Engine. Remote Sensing. 12(7): Article No. 1220. DOI: https://doi.org/10.3390/rs12071220

Story, M. and Congalton, R. (1986). Accuracy assessment: a user's perspective. Photogrammetric Engineering and Remote Sensing. 52 (3): 397- 399. Available at: https://www.asprs.org/wp-content/uploads/pers/1986journal/mar/1986_mar_397-399.pdf (Accessed on 10 June 2024)

Talukdar, S.; Singha, P.; Mahato, S.; Praveen, B.; Rahman, A. (2020). Dynamics of ecosystem services (ESs) in response to land use land cover (LU/LC) changes in the lower Gangetic plain of India. Ecol. Indic. 112, 106121. DOI: https://doi.org/10.1016/j.ecolind.2020.106121

Tamiminia H, Salehi B, Mahdianpari M, Quackenbush L, Adeli S, Brisco B. (2020). Google Earth Engine for geo-big data applications: A meta-analysis and systematic review. ISPRS Journal of Photogrammetry and Remote Sensing. 164: 152-70. DOI: https://doi.org/10.1016/j.isprsjprs.2020.04.001

Teluguntla, P.; Thenkabail, P.S.; Oliphant, A.; Xiong, J.; Gumma, M.K.; Congalton, R.G.; Huete, A. (2018). A 30-m Landsat-derived cropland extent product of Australia and China using random forest machine learning algorithm on Google Earth Engine cloud computing platform. ISPRS J. Photogramm. Remote Sens. 144, 325–340. DOI: https://doi.org/10.1016/j.isprsjprs.2018.07.017

Tewkesbury AP, Comber AJ, Tate NJ, Lamb A, Fisher PF. (2015). A critical synthesis of remotely sensed optical image change detection techniques. Remote Sensing of Environment, 160: 1-14. DOI: https://doi.org/10.1016/j.rse.2015.01.006

Vizzari M. (2022). PlanetScope, Sentinel-2, and Sentinel-1 data integration for object-based land cover classification in Google Earth Engine. Remote Sensing. 14(11): Article No. 2628. DOI: https://doi.org/10.3390/rs14112628

Woznicki, S. A., J. Baynes, S. Panlasigui, M. Mehaffey, and A. Neale. (2019). Development of a Spatially Complete Floodplain Map of the Conterminous United States Using Random Forest. Science of the Total Environment. 647: 942–953. DOI: https://doi.org/10.1016/j.scitotenv.2018.07.353

Zhang, C.; Sargent, I.; Pan, X.; Li, H.; Gardiner, A.; Hare, J.; Atkinson, P.M. (2019). Joint Deep Learning for land cover and land use classification. Remote Sens. Environ. 221, 173–187. DOI: https://doi.org/10.1016/j.rse.2018.11.014

تقييم تغيرات الغطاء الأرضي في محمية الأرز والشوح، سورية، باستخدام بيانات القمر الصناعي Sentinel 2A ومنصة Google Earth Engine

علا علي مرهج[1*]

[1] الهيئة العامة للاستشعار عن بعد– فرع المنطقة الساحلية. اللاذقية– سورية، محاضِرة في جامعة تشرين، اللاذقية، سورية.

(*للمراسلة: الباحث علا مرهج، البريد الإلكتروني: safaadakhil5@gmail.com ، هاتف: 0932044199)

تاريخ الاستلام: 6/ 2/ 2025 **تاريخ القبول:** 15/ 6/ 2025

الملخّص

أصبح التغير المتسارع في الغطاء الأرضي مشكلة كبيرة ناجمة عن عوامل مختلفة في محمية الأرز والشوح رغم وقوعها تحت الحماية. هدفت هذه الدراسة إلى تقييم مدى فائدة لرصد التغيرات في الغطاء الأرضي في محمية الأرز والشوح في سورية خلال فترة 5 سنوات الأخيرة (2018–2023) باستخدام صورتين من القمر الصناعي Sentinel-2 (S2) ملتقطتين في العامين 2018 و2023، ثم تطبيق نموذج (Random Forest "RF") ضمن منصة Google Earth Engine (GEE). أظهرت النتائج أن الدقة الإجمالية (Overall Accuracy (OA) للتصنيف في خرائط الغطاء الأرضي الناتجة بلغت 93.4% في خريطة 2018 و92.7% في خريطة 2023. من جهة أخرى، أظهرت الخرائط انخفاض الغطاء الغابوي في المحمية بنسبة 36.07% من إجمالي مساحة المحمية خلال فترة الدراسة. بالمقابل، تدعم النتائج بقوة استخدام منصة GEE وبيانات القمر الصناعي Sentinel 2A بالتوازي مع خوارزمية الغابة العشوائية لتعزيز دقة تصنيف الغطاء الأرضي في المناطق الجبلية. أوصت هذه الدراسة بضرورة اتخاذ إجراءات سريعة للحفاظ على الموارد الطبيعية النادرة في محمية الأرز والشوح.

الكلمات المفتاحية: تصنيف الصور، الغابة العشوائية، الاستشعار عن بعد، خرائط الغطاء الأرضي، الغابات، محمية الأرز والشوح، منصة Google Earth Engine.